

# The effect of heat treatment temperature on the properties of the composite duplex electroless coating of Ni-P/Ni-B-BN containing boron nitride nanoparticles

A. Baibordi<sup>1</sup>, K. Amini<sup>2\*</sup>, M. H. Bina<sup>3</sup>, A. Dehghan<sup>1</sup>

<sup>1</sup>*Materials Engineering Division, Shiraz University, Shiraz, Fars, Iran*

<sup>2</sup>*Department of Mechanical Engineering, Tiran Branch, Islamic Azad University, Isfahan, Iran*

<sup>3</sup>*Department of Advanced Materials and New Energies, Iranian Research Organization for Science and Technology, Tehran, Iran*

Received 12 April 2013, received in revised form 15 April 2014, accepted 2 May 2014

## Abstract

In this research, the effect of heat treatment on the hardness and wear resistance of the composite duplex electroless coating of Ni-P/Ni-B containing BN nanoparticles has been investigated. For this purpose, a 15-micron Ni-P electroless coating and a 10-micron Ni-B-BN electroless coating were applied on the surfaces of samples. The coated samples were heat treated for 1 h at 300, 400 and 500 °C. The effect of heat treatment on the morphology, hardness and wear behavior of the coatings was studied by the SEM, XRD, and pin-on-disc wear test. Tafel polarization test showed that the presence of the Ni-P electroless coating improves the corrosion resistance of the duplex coating. Moreover, the microhardness of coating was evaluated before and after the heat treatment via the Vickers microhardness testing machine to evaluate the effect of heat treatment temperature on the hardness of the samples. The results indicated that the produced coating morphology was cauliflower-shaped. The heat treatment at 400 °C creates the nano-crystalline structure, thereby increasing the hardness and wear resistance of the coating due to its change from the amorphous to crystalline structure and the production of the Ni<sub>3</sub>B hard phase. The Tafel polarization test revealed that the Ni-P layer improved the corrosion resistance of the two-layer composite coating.

**Key words:** nickel-boron electroless coating, heat treatment, corrosion, hardness, wear resistance

## 1. Introduction

Electroless coating has received special industrial attention due to its advantages, such as the production of an even coating without any need for electrical equipment for electroplating and any limit for the system volume [1]. The nickel electroless electroplating bath with the boron hydride reduction factor has recently received great attention. The properties of the nickel-boron electroless coating are mostly similar to those of the nickel-phosphorus electroless coatings. The major advantage of the boron-nickel electroless coating is its superiority of hardness and its wear resistance [2]. The presence of the secondary phase particles in these coatings improves some of

the properties of coating, including hardness and wear resistance. Due to their suitable lubricating properties, lack of solubility in most solvents, stability at relatively high temperatures, and low friction index, BN particles are added to coatings for tribological use as lubricants [3, 4]. The performing of heat treatment on nickel electroless coatings results in the nano-crystallization of coating and the production of hard phases, leading to an increase in hardness and wear resistance of these coatings [5]. The goal of this research is to produce the composite duplex electroless nickel-phosphorus/nickel-boron coating containing boron nitride nanoparticles and to investigate the effect of heat treatment on the properties of the produced coating.

\*Corresponding author: tel.: 00989131651659; e-mail address: [k\\_amini1978@iautiran.ac.ir](mailto:k_amini1978@iautiran.ac.ir)

## 2. Materials and methodology

### 2.1. Sample preparation

The CK45-steel disc-shaped samples with a thickness of 5 mm and a diameter of 50 mm were prepared and sand blasted by the 100-micro silicon particles. Sand blasting was performed on the samples before coating to improve the substrate adhesion. After the sand blasting operation, the samples were coated with the composite duplex electroless nickel-phosphorus/nickel-boron coating containing boron nitride nanoparticles (Ni-P/Ni-B-BN). The commercial SLO-TONIP 70A electroless solution produced by the German Shloter Company was used to provide the nickel-phosphorus electroless coating on the samples. The pH of this bath was 4.6 with a coating temperature of 85 °C. In order to produce the nickel-boron coating containing boron nitride nanoparticles, the boron-nickel electroless bath was first constructed. 20 g l<sup>-1</sup> nickel chloride, 1 g l<sup>-1</sup> sodium hydride, 56 g l<sup>-1</sup> ethylenediamine, 40 g l<sup>-1</sup> sodium hydroxide, and 0.01 g l<sup>-1</sup> lead nitride (pb<sup>2+</sup>) formed the chemical combination of this bath. Then, 5 g l<sup>-1</sup> of boron nitride powder (BN) was added to the bath and the bath was placed in an ultrasonic bath for 2 h so that these particles could uniformly be distributed inside the bath. The pH of the bath was considered to be 12.5 with the coating temperature of 85 °C. After the particles were evenly distributed, the coating operation started. In order to study the role of the nickel-phosphorus electroless coating in the Ni-P/Ni-B-BN composite duplex coating, the corrosion studies were conducted on this coating and compared with the Ni-B-BN and Ni-P single-layer coatings (with a similar thickness of 25 μm).

### 2.2. Electrochemical measurement

The studies related to the corrosion resistance of coatings were performed by the Tafel polarization test in the NaCl 3.5 % solution by the PARSTAT 2273 device. The samples with the surface area of 1 cm<sup>2</sup> were put in contact with the electrolyte. The platinum electrode and the saturated calomel electrode (SCE) were employed as the standard electrode and the reference electrode, respectively. By use of the Tafel extrapolation method, the potential and corrosion current density were extracted from the Tafel curves. The surface roughness was evaluated via a roughness testing machine (Mitutoyo-sj-201). For this purpose, the roughness was evaluated for at least 5 times in each sample to evaluate an accurate average value.

### 2.3. Surface analysis and characterization

The bending test was also carried out to clarify

the effect of the surface preparation on the coating adhesion with respect to the ASTM B97-571. Regarding this standard, a smaller crack in the fillet areas improved the adhesion. Moreover, should the coating be disbanded easily, it can be clarified that the adhesion is not sufficiently strong. For further studies, the samples surface was analyzed at 30× magnification via the scanning electron microscope. A line with a 40 mm length was then drawn in the micrographs and the number of cracks cutting the line was evaluated. The distance between the cracks was then calculated regarding Eq. (1):

$$\begin{aligned} \text{Average distance between cracks} &= \\ &= \frac{40 \text{ mm}}{\text{Number of cracks}} \end{aligned} \quad (1)$$

To investigate the effect of heat treatment temperature on the composite duplex coating, some of the samples were coated and heat treated at 300, 400, and 500 °C for 1 h in the inert atmosphere (argon gas). Ultimately, the scanning electron microscope and the X-ray diffraction device were used to study the morphology of the surface of the samples and the phase analysis at the surface of the samples, respectively. The crystal sizes were evaluated using the Sherre method and the X'Pert High Score Version 1.0d software. The hardness of the samples was also measured on a micro scale with the initial weight of 100 g through the Vickers method with respect to the ASTM B733 standard. For more accuracy, the hardness was evaluated for at least 5 times in similar samples to evaluate a reliable average value.

The pin-on-disc wearing machine was used to evaluate and compare the tribological behavior of the samples. In all the wearing tests, the 52100 steel pin with a hardness of about 65RC and a diameter of 6 mm was used as an abrasive. The wearing test was performed in the air atmosphere at the sliding rate of 0.1 ms<sup>-1</sup> under the 5 N force and the maximum sliding distance of 1000 m.

## 3. Results and discussion

### 3.1. Effect of surface preparation on the coating adhesion

The sand blasted samples showed the lowest crack distance and hence the height adhesion, as compared with the other samples (Table 1). The average value of the substrate roughness was 1.31 μm. The sand blasted samples showed the lowest crack distance and hence the height adhesion, as compared with the other samples. The average roughness value in the sand blasted substrate was 1.31 μm and at the ground surfaces (the 600-emery paper) was 0.62 μm. Increasing

Table 1. The number of cracks and the average values of their distances in the adhesion test

Coating	Type of substrate preparation	Number of cracks	Average distance between cracks
Ni-P	sand blasted samples	29	1.4
	600 emery paper	16	2.5
Ni-P/Ni-B-BN	sand blasted samples	24	1.7
	600 emery paper	14	2.9
Ni-B-BN	sand blasted samples	8	5
	600 emery paper	*	*

\*The coating was disbanded from the substrate

the surface roughness improved the adhesion of the coating to the substrate. Moreover, it was shown that the Ni-P layer in the two-layer composite coating improved the adhesion greatly. Regarding the adhesion test results, the coated layer in the sand blast substrate was used for further investigations.

### 3.2. Study of the morphology and the coating cross-section

The morphology and the Ni-P/Ni-B-BN composite duplex electroless coating cross-section produced on the steel-substrate are shown in Fig. 1. Figure 1 shows that the coating morphology is cauliflower in shape, which is common in boron-nickel electroless coatings [2]. As can be seen in this figure, BN nanoparticles have been able to set in the Ni-B matrix and the matrix still enjoys the proper adhesion. Figure 1b shows that the Ni-P/Ni-B-BN composite duplex electroless coating deposited on the substrate is highly even and shows a good connection to the substrate. The thickness of the Ni-P layer in the duplex coating is about 15  $\mu\text{m}$  and of the Ni-B-BN layer is about 10  $\mu\text{m}$ .

### 3.3. The role of the nickel-phosphorus electroless layer in duplex coating

The role of the nickel-phosphorus electroless layer produced on the duplex coating was studied by the Tafel polarization test. Table 1 shows the potential and rate of the Ni-P/Ni-B-BN composite duplex coating corrosion, as well as the Ni-B-BN and Ni-P mono-layer coatings extracted from the Tafel polarization curves. This table shows that the Ni-P electroless coating enjoys the most positive ( $E_{\text{corr}}$ ) corrosion potential and the lowest ( $i_{\text{corr}}$ ) current corrosion density among the curves under study. Also, the Ni-P/Ni-B-BN composite duplex coating shows more positive corrosion potential and a severe reduction in the corrosion current density, as compared to the Ni-B-BN composite single-layer coating. When corrosion takes place on the

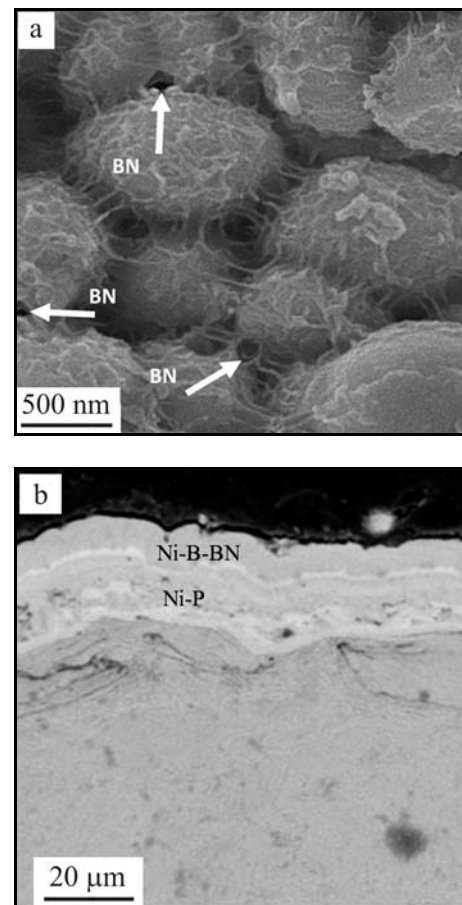


Fig. 1. Images taken by scanning electron microscope: surface (a) and Ni-P/Ni-B-BN duplex coating of the cross-section (b).

Ni-B-BN composite duplex coating, some of the produced voids expand toward the gravity force and reach the Ni-P inner layer. Since the exterior Ni-B-BN layer enjoys more negative corrosion potential with higher corrosion current density, as compared to the Ni-P layer, it is corroded more easily and acts as a sacrifi-

Table 2. The potential and density of the corrosion current resulting from the Tafel polarization curves

Coating	$E_{\text{corr}}$ (mV)	$i_{\text{corr}}$ ( $\mu\text{A cm}^{-2}$ )
Ni-P	-300	1.6
<b>Ni-P/Ni-B-BN</b>	<b>-430</b>	<b>4.5</b>
Ni-B-BN	-570	50

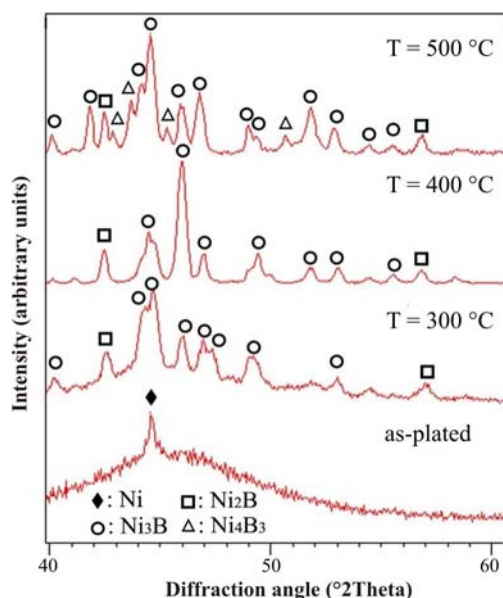


Fig. 2. Effect of heat treatment temperature on Ni-P/Ni-B-BN coating X-ray diffraction pattern.

cial anode for the Ni-P layer. Therefore, it lengthens the life span of the Ni-P layer and subsequently the steel substrate. On the whole, the nickel-phosphorus layer increases the corrosion resistance of the composite duplex coatings (Table 2) [7].

### 3.4. The effect of heat treatment temperature on the coating structure

Figure 2 shows the electroless coating X-ray diffraction pattern before and after heat treatment. This figure shows that the produced coating contains a mixture of amorphous and crystalline microstructure before heat treatment. As it is observed, the surface of the heat treated coating is indicative of a complete change in the structure relative to its raw state. In other words, instead of amorphous effects, the clear peaks of the two phases of crystalline nickel with FCC lattice and  $\text{Ni}_3\text{B}$  nickel boron with orthorhombic crystalline lattice are observed in diffraction diagrams. As shown below, increasing the temperature causes an increase in the intensity of Ni and  $\text{Ni}_3\text{B}$  peaks in the

Table 3. The effect of heat treatment temperature on the coatings hardness

Coating	Heat treatment temperature ( $^{\circ}\text{C}$ )	Hardness HV
Substrate	non-heat treated	220
Ni-P	non-heat treated	600
Ni-P	400	973
Ni-P/Ni-B-BN	non-heat treated	705
Ni-P/Ni-B-BN	300	941
Ni-P/Ni-B-BN	400	1449
Ni-P/Ni-B-BN	500	1022

XRD pattern. The best crystallization temperature is  $400^{\circ}\text{C}$  and by an increase in temperature ( $500^{\circ}\text{C}$ ), the grains grow and the presence of ( $\text{Ni}_4\text{B}_3$ ) unwanted phases is observed in the coating [5]. The average crystal size of the heat-treated Ni-P/Ni-B-BN coating at 300, 400 and  $500^{\circ}\text{C}$  was 42, 26 and 39 nm, respectively. The results showed that heat treatment at  $400^{\circ}\text{C}$  resulted in the crystallization of the coating [4].

### 3.5. Effect of heat treatment temperature on coating hardness

The results obtained from the microhardness test (Table 3) showed that the highest hardness belonged to the heat treated Ni-P/Ni-B-BN composite duplex coating at  $400^{\circ}\text{C}$ . Studies showed that the hardness increase was related to more deposit of the  $\text{Ni}_3\text{B}$  intermetallic stable phase during the amorphous phase crystallization [5]. The coating hardness at  $300^{\circ}\text{C}$  is decreased due to the initiation of crystallization and the simultaneous presence of the amorphous and crystalline structure at  $500^{\circ}\text{C}$  due to an increase in temperature and excess growth of the  $\text{Ni}_3\text{B}$  grains, as well as the formation of the unwanted  $\text{Ni}_4\text{B}_3$  phases relative to hardness at  $400^{\circ}\text{C}$ . These results are in a good agreement with the XRD results. Furthermore, the BN nanoparticles as the secondary phase in the coating produce the Ni-P/Ni-B-BN composite coating, thereby improving the hardness further, as compared with the Ni-P electroless coating.

### 3.6. Effect of heat treatment temperature on wear behavior of the coating

With regard to the results of the admissibility load test, wearing tests were performed under a 5 N force. The weight reduction curves of the samples in terms of the sliding distance in ambient conditions are shown in Fig. 3. The weight loss diagram for the Ni-P coating is also drawn. As it is observed, the heat treated samples at  $400^{\circ}\text{C}$  experience the minimum weight reduction and the samples without heat treatment ex-

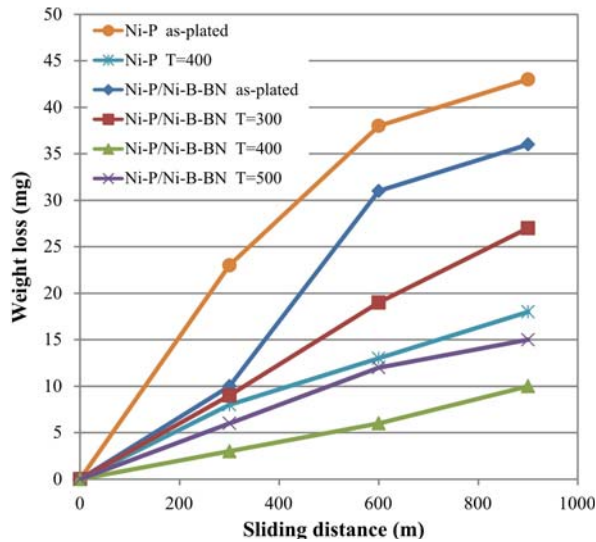


Fig. 3. Weight reduction diagrams in terms of Ni-P/Ni-B-BN coating travelled distance.

perience the maximum weight reduction. This conclusion relates to the  $\text{Ni}_3\text{B}$  intermetallic stable phase sediment during the amorphous phase crystallization and is provable using the XRD and microhardness test results. This behavior is also a consequence of the lubricating effect of the BN nanoparticles [6].

Figure 4 shows the images of the abraded surfaces of the Ni-P/Ni-B-BN coating obtained by the scanning electron microscope before and after heat treatment at  $400^\circ\text{C}$ . As it is observed in Fig. 4a, due to the low hardness of the coating and lack of crystalline phase formation before heat treatment, the sample abraded surface results in the intensification of plastic deformation in the coating. The plastic deformation, the creation of local fittings at contact regions, and the rupture of these fittings are a result of the continuation of sliding distance; therefore, the dominant mechanism in the abrasion of this sample is the abrasive wear [6].

Figure 4b shows that heat treatment at  $400^\circ\text{C}$  for 1 h results in changing the amorphous structure into crystalline nickel and  $\text{Ni}_3\text{B}$ , leading to a reduc-

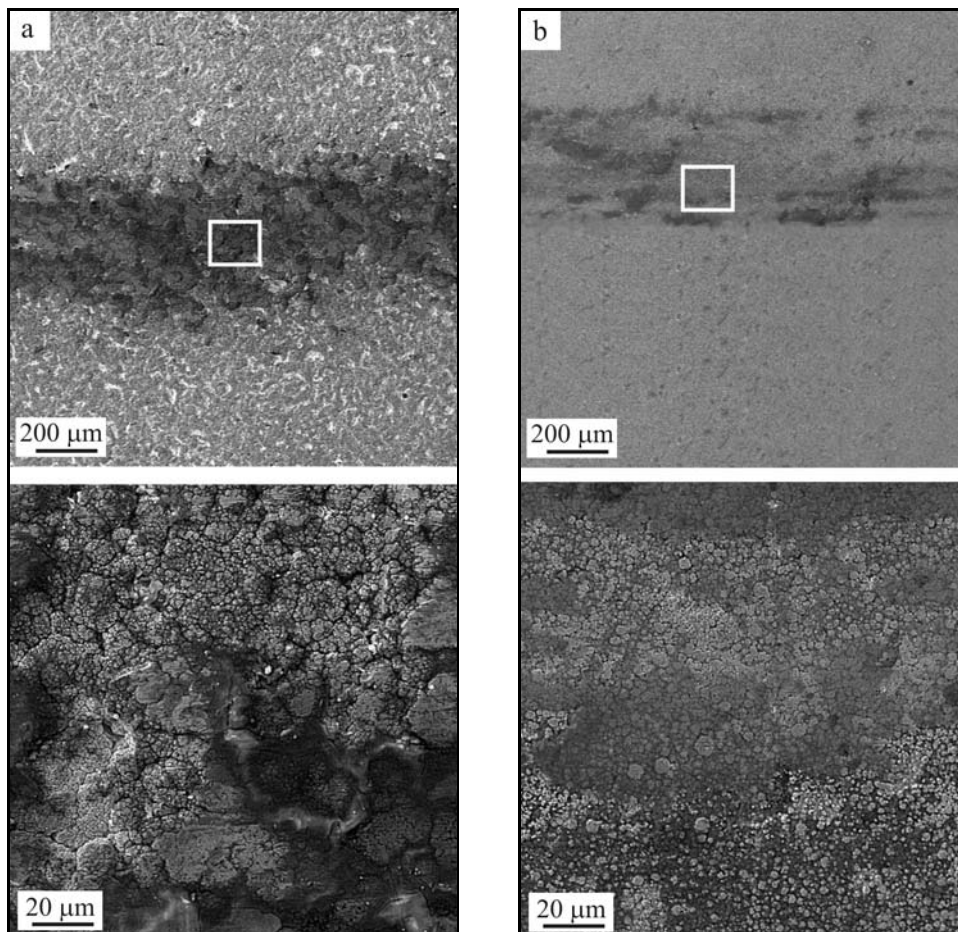


Fig. 4. Taken images by scanning electron microscope of abraded surfaces of Ni-P/Ni-B-BN before heat treatment (a) and after heat treatment at  $400^\circ\text{C}$  for 1 h (b).



tion in the abraded surface. The SEM image of this sample showed that the Ni-P/Ni-B-BN composite duplex coating remained on the surface of this sample even after 1000 m of sliding distance.

#### 4. Conclusion

In this study, the dual composite electroless coating of Ni-P/Ni-B-BN was coated on a substrate of CK45 steel, and the following results were obtained:

1. The semi-amorphous Ni-P/Ni-B-BN duplex electroless coating is cauliflower in shape.

2. Since the corrosion resistance of Ni-B-BN is low, a dual layer coating, which has high corrosion resistivity because of the Ni-P substrate, has been used.

3. Heat treatment at 400 °C creates the nano-crystalline structure, resulting in an increase in the hardness and wear resistance of the coating due to a change from the amorphous to crystalline structure and the creation of the Ni<sub>3</sub>B hard phase.

4. Grain growth at 500 °C and lack of complete and homogeneous nano-crystalline structure at 300 °C are the main causes of decreasing the wear resistance of coating in comparison with 400 °C.

#### References

- [1] Tenno, R.: Electroless Nickel Plating. Stevenage, Hertfordshire, Finishing Publications LTD 1991.
- [2] Duncan, R. N., Arney, T.: *Plat Surf Finish.*, 71, 1984, p. 49.
- [3] Leon, O. A., Staia, M. H., Hintermann, H. E.: *Surf Coat Tech.*, 120–121, 1999, p. 641.
- [4] Leon, O. A., Staia, M. H., Hintermann, H. E.: *Surf Coat Tech.*, 163–164, 2003, p. 578.  
[doi:10.1016/S0257-8972\(02\)00663-1](https://doi.org/10.1016/S0257-8972(02)00663-1)
- [5] Chen, C. K., Feng, H. M., Lin, H. C., Hon, M. H.: *Thin Solid Films*, 416, 2002, p. 31.  
[doi:10.1016/S0040-6090\(02\)00628-4](https://doi.org/10.1016/S0040-6090(02)00628-4)
- [6] Abdel Hamid, Z., Hassan, H. B., Attyia, A. M.: *Surf Coat Tech.*, 205, 2010, p. 2348.  
[doi:10.1016/j.surfcoat.2010.09.025](https://doi.org/10.1016/j.surfcoat.2010.09.025)
- [7] Biestek, T.: *Galvanotechnic*, 88, 1997, p. 1488.